Time-dependent radiative transfer in magneto-optical traps

N. N. Bezuglov,[1] A. F. Molisch,[2] A. Fioretti,[3,4] C. Gabbanini,[3] F. Fuso,[4] and M. Allegrini[4]
[1]*V. A. Fock Institute of Physics, St. Petersburg University, Ulianovskaya 1, 198904 St. Petersburg, Russia*
[2]*Department of Electroscience, Lund Technical University, Ole Romer Waeg 3, Lund, Sweden*
[3]*Istituto per i Processi Chimico-Fisici del CNR, Via Moruzzi, I-56124 Pisa, Italy*
[4]*INFM, Dipartimento di Fisica Enrico Fermi, Università di Pisa, Via F. Buonarroti 2, I-56127 Pisa, Italy*
(Received 14 June 2002; revised manuscript received 30 June 2003; published 31 December 2003)

We investigate radiation-imprisonment (RI) phenomena in a system of cold atoms trapped in magneto-optical traps (MOTs) when cooling lasers are switched off for a short period. The problem is formulated within the framework of the Streater-Cooper-Sandle equation that belongs to the Markov class and accounts for photon frequency redistribution in multiple scattering processes. On the basis of a semiclassical approach, we derive explicit analytical solutions for the spectral problem of the RI equation neglecting Doppler effects. The analysis reveals peculiarities in emission profiles under initial partial saturation of the resonance transition by the probe laser pulse. Comparison between theoretical and experimental data on effective radiative lifetimes obtained in Cs and Rb MOTs confirms the validity of the discussed nonstationary model of RI in cold samples. For small detunings, the Streater-Cooper-Sandle equation agrees with the experimental data, while in the case of large detunings, the theory does not agree, probably due to non-Markovian effects.

DOI: 10.1103/PhysRevA.68.063415 PACS number(s): 32.80.Pj, 32.50.+d, 03.65.Sq

I. INTRODUCTION

Radiation imprisonment (RI) in atom systems represents an important issue in a wide range of atomic physics and spectroscopy experiments [1]. The sequence of multiple absorption/reemission processes leads to remarkable effects on both intensity [2] and temporal behavior [3,4] of the fluorescence emitted by atomic samples (see also Ref. [1,5]). In the past years, large efforts have been devoted to the study of atom systems cooled down to temperatures in the nanokelvin and microkelvin range, and, more recently, to the attainment of Bose-Einstein condensation of atoms. RI in laser cooled systems represents an interesting topic due to two fundamental reasons. First, the specific properties of cold atoms (reduced Doppler width, relatively large atom density, controlled preparation of atomic states) are a fascinating field for the investigation of multiple scattering of light [6]. Moreover, RI plays a fundamental role in the trapping and cooling mechanisms, providing an important heating and loss channel [7] for trapped atoms, which prevents the attainment of arbitrarily low temperature and high density of the samples [8].

RI in steady-state conditions is described by comparatively well established and closed theories [2]. However, in cold regimes the situation dramatically changes for time-dependent dynamics: the lack of a wide Doppler broadening leads, formally, to complicated retardation terms [2] in the kinetic equations that determine the evolution of the ''atom + photon'' interacting system. There are, nevertheless, important problems when radiative transfer may be considered as a nearly Markov process, i.e., being quasi-local-in-time. Under interaction with laser radiation, ground states are radiatively broadened with the width Γ' [9]

$$\Gamma' \simeq \frac{s}{1+2s}\Gamma, \quad s=\frac{\Omega^2}{\Gamma^2+4\delta^2}, \tag{1}$$

resulting in the linewidth $\Delta\omega_{fl} \simeq \Gamma'$ of the fluorescence signal. Here Γ is the natural width of the excited level, s denotes the saturation parameter for laser light detuned by the quantity $\delta=\omega_L-\omega_0$ (angular frequency units) from the line center, and Ω is the corresponding Rabi frequency. The time $\tau_{sc}=1/\Gamma' \simeq 1/\Delta\omega_{fl}$ for photon scattering by an atom [9,10] is to be compared with the characteristic time τ_{ef} of RI, i.e., the decay time of the excited-state population. We note that τ_{ef} and τ_{sc} can be varied independently in the experiment, by changing the optical thickness of the sample and the intensity and detuning of the probe laser used to excite the fluorescence, respectively, as it will be discussed in Sec. II.

The key point of our RI treatment is that when τ_{ef} exceeds the scattering time τ_{sc} one can consider the situation as quasi-steady-state, i.e., neglect the retardation effects. It becomes possible then to apply the theoretical model that will be introduced in Sec. III, treating coherent Rayleigh scattering as a process local in time [11,12]. Moreover, as the solutions for decaying modes of the RI equation presented in Sec. IV preserve the initial emission profile broadening $\Delta\omega_{fl}$ on the level of $\Gamma/2$ units, the present theoretical treatment is approximately valid even at the decaying stage of the experiment. In other words, it is enough to have the condition $\tau_{ef} \gg \tau_{sc}$ fulfilled *only* at the beginning of the afterglow process. This fact provides validity for the evaluation of photon trapping factors according to the proposed RI model, and explains the agreement between experimental data and theory predictions for small detunings of the probe laser (see Sec. V). On the other hand, we demonstrate a discrepancy between experiment and theory occurring in the case of large detunings, i.e., when the criterion $\tau_{ef} \gg \tau_{sc}$ is not fulfilled during the excitation stage.

II. EXPERIMENT

In the present work we analyze RI in the fluorescence emission from Rb and Cs magneto-optical traps (MOTs) that have been realized in two separate setups (see Refs. [13] and [14], respectively, for more detailed descriptions). In them,

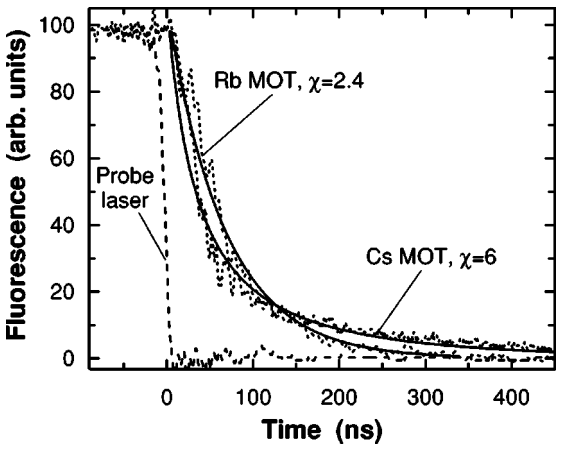

FIG. 1. Fluorescence decay signals (dotted lines) for Cs and Rb MOTs (as marked close to each curve). Solid lines superimposed on experimental data represent theoretical results obtained as discussed in the text (Sec. V). The dashed line is the time behavior of the falling edge of the probe laser pulse, shown as a reference.

samples of nearly 10^7–5×10^8 atoms can be stored at temperatures in the 100–400 μK range, and at densities in the 10^{10}–10^{11} cm^{-3} range. We note that, in a similar density range, atomic wave functions are not overlapping, so that individual atom scattering processes can be considered.

In a typical experimental sequence the MOT is loaded with the cold sample for a period of about 10–50 ms and then the trapping laser beams are shut off for a few millisecond by means of acousto-optical and mechanical shutters. As the repumping laser is left on during the whole cycle, the trapped atoms can be considered as being all in the upper hyperfine level of the ground state ($F=3$ for ^{85}Rb and $F=4$ for Cs). During the dark period, they do not interact anymore with the repumper beam and start falling ballistically under the influence of gravity. After ≈ 80 μs in the dark, cold atoms are excited by a nearly rectangular probe laser pulse with a duration in the 300–1600 ns range (the fall time of the pulse being shorter than the natural lifetime $1/\Gamma$ of the excited level) attained by electro-optic modulation of a cw probe diode laser. The probe laser, whose saturation parameter s could be varied in the range $s=1/3$–3, was resonant with the $6S_{1/2}(F=4)\rightarrow 6P_{3/2}(F'=5)$ D_2 transition in the Cs case while it could be accurately tuned around the corresponding $5S_{1/2}(F=3)\rightarrow 5P_{3/2}(F'=4)$ transition for ^{85}Rb. Due to the specific operating conditions of the two experiments, the opacity of the cold sample could be varied in the range $\chi\sim 5$–12 in the Cs MOT [13], whereas Rb measurements were taken at a fixed value $\chi=2.4$. The decay of the MOT fluorescence, excited by the probe laser pulse, was observed by a fast photomultiplier, and recorded on a digital oscilloscope after averaging over several hundred shots.

Typical signals at zero detuning of the probe laser are plotted in Fig. 1 for Rb and Cs traps ($\chi=2.4$ and $\chi=6$, respectively). To extract the effective decay time τ_{ef} from the experimental findings, we adopted the criterion of fitting to a single exponential function the recorded signal starting from the time which corresponds to a fluorescence intensity equal to 1/3 of its maximum value. For the signals reported in the figure, the criterion leads to consider data for a time greater than nearly 55 ns and 75 ns for Cs and Rb, respectively. As it will be discussed in Sec. IV, this procedure ensures that contribution of higher modes is practically negligible.

III. MASTER EQUATION OF RI

All during the excitation by the probe laser pulse, our experimental conditions generally ensure that the inequality $\tau_{ef}>\tau_{sc}$ is satisfied. In Sec. V we will demonstrate that such inequality corresponding to a quasi-steady-state regime of RI holds also in the fluorescence decay stage, when no external radiation is applied to the sample. As a consequence, RI takes place in the range of validity of the Streater-Cooper-Sandle (hereafter denoted as SCS) equation [11], describing the evolution of the emissivity $N(\vec{r},\nu,t)$ of excited atoms related to the spatial coordinate $\vec{r}$ and the frequency ν. The corresponding evolution equation, which is thus the basic ingredient of our treatment, reads

$$\frac{\partial N(\vec{r},\nu,t)}{\partial t}=-\Gamma N(\vec{r},\nu,t)+S_\nu(\vec{r},t)+\overline{\kappa}\int_{-\infty}^{\infty}d\nu'\int_\Omega d^3r'\tilde{G}_{\nu'}(|\vec{r}-\vec{r}'|)\times\left\{\Gamma R_{\nu\nu'}+\left[R_{\nu\nu'}-\frac{\kappa(\nu)\kappa(\nu')}{\overline{\kappa}^2}\right]\frac{\partial}{\partial t}\right\}\times N(\vec{r}',\nu',t). \quad (2)$$

The product $\Gamma N(\vec{r}',\nu',t)d^3r'd\nu'$ gives the amount of photons spontaneously emitted per second within the frequency interval $[\nu';\nu'+d\nu']$ by the excited atoms contained in the volume d^3r'. The propagator $\tilde{G}_{\nu'}(\rho)=\exp[-\rho\kappa(\nu')]/(4\pi\rho^2)$ describes the photon transfer from an emitting atom (located at the point $\vec{r}'$) to an absorbing one (located at the point $\vec{r}$), while $R_{\nu\nu'}$ is the angle-averaged frequency redistribution function. The spectral functions $R_{\nu\nu'}$, $N(\vec{r},\nu,t)$ satisfy the normalization conditions

$$\overline{\kappa}\int_{-\infty}^{\infty}d\nu R_{\nu\nu'}=\kappa(\nu'),\qquad \int_{-\infty}^{\infty}d\nu N(\vec{r},\nu,t)=n^*(\vec{r},t), \quad (3)$$

where $\kappa(\nu)$ is the spectral absorption coefficient with $\overline{\kappa}\equiv\int_{-\infty}^{\infty}d\nu\kappa(\nu)$ and $n^*(\vec{r},t)$ is total density of excited atoms at the point $\vec{r}$. The source term $S_\nu(\vec{r},t)$ accounts for nonradiative level excitation (e.g., via collision or/and cascade processes). We note that the original SCS equation deals with the angle-averaged emission coefficient $\eta(\vec{r},\nu,t)$ which, after simple rescaling [see Eq. (20a) in Ref. [11]] is reduced to the frequency-dependent density function entering Eq. (2): $N(\vec{r},\nu,t)=4\pi/(\Gamma h\nu)\,\eta(\vec{r},\nu,t)$. Because of the normalization property, Eq. (3), the function $N(\vec{r},\nu,t)$ is in widespread use in physical literature [1,15,16]. We call attention also to the fact that Eq. (2) differs from the evolution equation de-

rived by Payne *et al.* [15] (hereafter referred as Payne equation) for the presence of the additive term in square brackets in the integrand.

Under MOT conditions, i.e., at low temperatures, we assume an absorption line shape described by the Lorentzian function

$$\kappa(\nu)=\kappa^{(L)}(\nu)\equiv\frac{\kappa_0^{(L)}}{1+\nu^2},\quad \kappa_0^{(L)}=\frac{\lambda^2}{2\pi}N\frac{\overline{g_1}}{\overline{g_2}},\tag{4}$$

with $\kappa_0^{(L)}$ the absorption coefficient at line center, the dimensionless reduced frequency ν being measured from the line center ν_0 in units of the Lorentz width, $\Delta\nu^{(L)}=\Gamma/4\pi$, λ the optical transition wavelength, $\overline{g_1}/\overline{g_2}$ the ratio of the statistical weights of excited and ground levels, and N the density of the ground level. Indeed, in typical MOT experiments, radiative broadening is much larger than Doppler broadening, $\Delta\nu^{(L)}/\Delta\nu^{(D)}\geqslant 20$ [13,14], so that we can neglect any Doppler effect. Thus, we can regard the redistribution function $R_{\nu\nu'}$ as essentially coherent due to the pure natural broadening:

$$\overline{\kappa}R_{\nu\nu'}=\delta(\nu-\nu')\kappa(\nu').\tag{5}$$

Directly measured effective radiative rate constants are connected with the so-called trapping (or Holstein) g_j factors [17]. These factors are associated with eigenvalues for the spectral problem of the radiation imprisonment equation [17]: $N(\vec{r},\nu,t)=\Psi_j(\vec{r},\nu)\exp(-\Gamma t/g_j)$. Eigenmodes Ψ_j and eigenvalues $\lambda_j=g_j^{-1}$ can be obtained from Eq. (2) by setting $\partial/\partial\, t\to-\Gamma\lambda_j$ and omitting the source function S_ν:

$$\lambda_j\Psi_j(\vec{r},\nu)=\Psi_j(\vec{r},\nu)-\overline{\kappa}\int_{-\infty}^{\infty}d\nu'\int_\Omega d^3r'\tilde{G}_{\nu'}(|\vec{r}-\vec{r}'|)\times\left\{R_{\nu\nu'}-\lambda_j\left[R_{\nu\nu'}-\frac{\kappa(\nu)\kappa(\nu')}{\overline{\kappa^2}}\right]\right\}\Psi_j(\vec{r}',\nu').\tag{6}$$

The factor g_j determines the effective rate of absorption/reemission processes for a photon in the jth mode. The fundamental mode corresponds to $j=0$. In this case, $g_0=\Gamma\tau_{ef}$.

IV. EMISSION PROFILES AND TRAPPING FACTORS IN THE MOTS

In previous works [18,19], we have developed a semiclassical approach, the geometrical quantization technique (GQT), to construct a complete set (spectrum) of Ψ_j and g_j for a wide class of integral transport equations, which allows us to analytically solve Eq. (2) via the Fourier method [1,17]. In the following, we outline the main points in exploiting GQT to solve RI problems in cold samples. We model the MOT as a uniform sphere of atoms [$N(r)=N_0$ for $r\leqslant R$] with volume $\Omega_{\rm Sh}$ and radius R. We note that, for MOTs in the multiple scattering regime [7], this is closer to reality than taking a Gaussian distribution of the absorption coefficient [$\kappa_0^{(Gau)}(r)=\kappa_0^{(Gau)}\exp(-r^2/R^2)$].

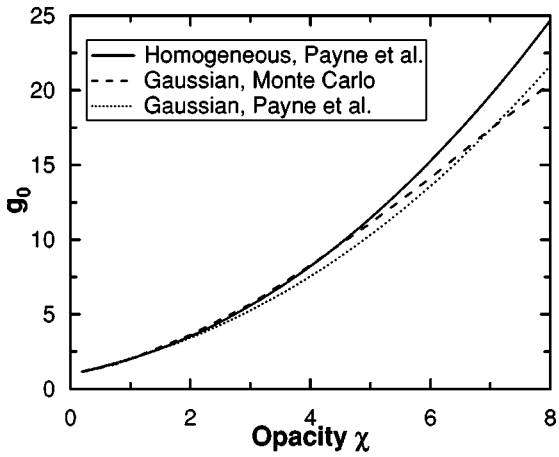

FIG. 2. Trapping factor g_0 for the fundamental mode as a function of the MOT opacity χ calculated for two different geometries (spherical homogeneous and Gaussian, solid and dotted lines, respectively) according to the modified GQT method of Ref. [20]. The dashed line corresponds to trapping factors extracted from a best fit of Monte Carlo simulations [13] for a Gaussian distribution of atoms. In all data, zero detuning of the probe laser is considered while the RI model is based on the equation of Payne *et al.* [15] with coherent redistribution function, Eq. (5).

In any case, we have estimated the discrepancy between the two geometries by employing both the approximate evaluation methods of Ref. [3] and the modified GQT of Ref. [20], specifically developed for studying RI in a space inhomogeneous absorbing medium, and based on the Holstein/Payne equations [15,17]. The results are shown in Fig. 2, where the g_0 factors evaluated for spherical homogeneous and Gaussian space distributions of atoms are reported as solid and dotted lines, respectively. The comparison suggests that, for the same opacity $\chi\equiv\int_0^\infty dr\,\kappa_0^{(Gau)}(r)=\kappa_0 R$, the values of the trapping factor for the Gaussian case exceed those corresponding to the homogeneous case by less than a factor $1+(2\pi+1)^{-1}$. The same figure reports also the g_0 factors obtained by a Monte Carlo simulation of RI in a spherical Gaussian MOT (dashed line). Details of the numerical method are discussed elsewhere [13]; g_0 values have been derived from simulation of the fluorescence decay by adopting the same criterion used in the analysis of the experimental signals (see Sec. II).

In solving the general spectral problem, Eq. (6), we shall restrict ourselves to spherically symmetrical modes depending on $r=|\vec{r}|$. It is convenient to present Ψ_j in a parametric form based on the factorization [19]:

$$\Psi_j(r,\nu)\simeq\varphi_j(\nu)n_j^*(r),\quad n_j^*(r)=\int_{-\infty}^{\infty}\Psi_j(r,\nu)d\nu,\tag{7}$$

where $n_j^*(r)$ is the total density of excited atoms in the mode j at radial distance r. Equation (7) implies an approximate separation of space and frequency variables. Because of this separation, the frequency part of the problem, i.e., the emission profile $\varphi_j(\nu)$, can be obtained for the easiest space configuration, an *infinite* R^3 coordinate space Ω_∞, where the modes have the explicit space representation: $n_p^*(r)$

$=\exp(ipr)$. It is noteworthy that the Fourier parameter p in R^3 plays the role of the mode indices j. The corresponding spectral problem in the frequency domain with the lineshape and the redistribution function of Eqs. (4) and (5), respectively, reads as

$$V_p(\nu)\varphi_p(\nu)=\frac{\lambda_p}{1-\lambda_p}\frac{\pi^{-1}}{1+\nu^2}\int_{-\infty}^{\infty}dx[1-V_p(x)]\varphi_p(x),$$

$$V_p(\nu)=1-\kappa^{(L)}(\nu)p^{-1}\arctan[p/\kappa^{(L)}(\nu)], \tag{8}$$

$[1-V_p(\nu)]/\kappa^{(L)}(\nu)$ being the Fourier transform of the kernel function $\tilde{G}_{\nu'}$ entering Eqs. (2) and (6).

As in Ω_∞ the spatial dependence $\exp(ipr)$ of the modes has the form of a wave function of some freely moving particle (an associated quasiparticle in the notation of Ref. [19]), the parameter p may be interpreted as its momentum [21]. Under such interpretation the spectral equation (6) acquires meaning [19] of some generalized stationary Schrödinger (wave) equation determining eigenfunction (modes) Ψ_j and eigenvalues (effective rate constants) λ_j of the quasiparticle.

The frequency spectral problem, Eq. (8), has simple solutions

$$\lambda_p^{-1}=\frac{1}{\pi}\int_{-\infty}^{\infty}\frac{d\nu}{1+\nu^2}\frac{1}{V_p(\nu)},\quad \varphi_p(\nu)=\frac{\lambda_p}{\pi}\frac{1}{1+\nu^2}\frac{1}{V_p(\nu)}. \tag{9}$$

This allows us to find explicit forms of both the emission profile $\varphi_p(\nu)$ and the effective radiative constant λ_p as functions of p. On the other hand, the dependence of $\Gamma\lambda_p$ on the momentum p determines the quasiparticle dispersion law, which, as discussed in detail in Ref. [19], plays the role of the quasiparticle kinetic energy.

Thus, considering an infinite volume enables derivation of the quasiparticle Hamiltonian $H(\vec{p},\vec{r})=\Gamma\lambda_p$, i.e., determining its dynamical properties. In our experimental conditions, however, we obviously have a *finite* sample volume. In other words, the quasiparticle is confined in the volume Ω_{Sh} [19]. As a consequence, its momentum p (the mode indices) acquires a discrete set of values p_j while $n^*_{p_j}(r)$ satisfies [19] the conventional Holstein spectral equation [17]

$$\lambda_j n^*_{p_j}(r)=n^*_{p_j}(r)-\int_{\Omega_{\mathrm{Sh}}}d^3r' n^*_{p_j}(r')\times\int_{-\infty}^{\infty}d\nu'\varphi(\nu')\kappa^{(L)}(\nu')\tilde{G}_{\nu'}(|\vec{r}-\vec{r}'|), \tag{10}$$

with the emission profile $\varphi(\nu)$ equal to $\varphi_{p=p_j}(\nu)$ [22]. At the same time, the decay constants $\Gamma\lambda_j$ of the modes coincide with the quantized energy values $\Gamma\lambda_{p=p_j}$ of the quasiparticle. Thus, the relevant momentum p_j turns out to be the characteristic of the spatial part of the problem and can be determined within GQT by using the Bohr-Sommerfeld quantization rules for the quasiparticle confined into Ω_{Sh} [18]:

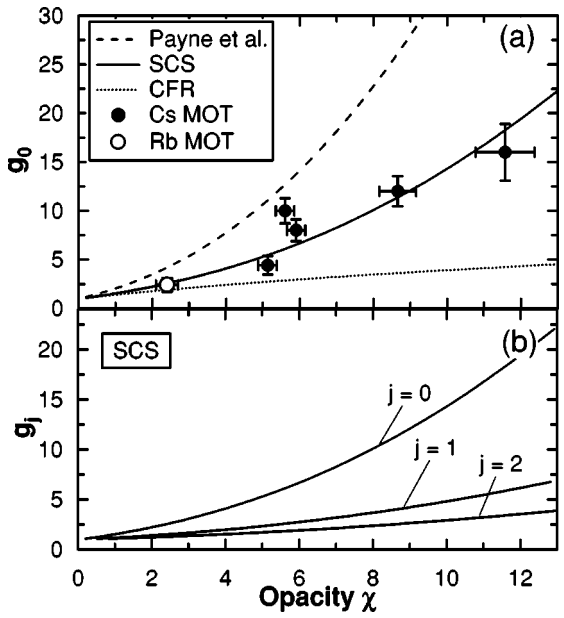

FIG. 3. (a): Trapping factor g_0 for the fundamental mode as a function of the MOT opacity χ, calculated according to three different RI models, as indicated in the legend. Experimental data obtained under excitation of the whole MOT volume with zero detuning are shown in the case of Rb and Cs MOTs (open and closed circles, respectively). (b): Trapping factors g_j for the first three modes ($j=0,1,2$) calculated as a function of the MOT opacity χ according to the SCS model.

$$2\frac{p}{\kappa_0^{(L)}}\kappa_0^{(L)}R=2\pi j+\Delta S(p)+\pi \tag{11}$$

with

$$\Delta S(p)=\frac{\pi}{2}\left[1+\frac{1}{2}p\frac{d}{dp}\ln\left(p\frac{d\lambda_p}{dp}\right)\right].$$

The mode index (quantum number) $j=\{0,1,2,\ldots\}$ fixes "permitted" values of the momentum $p_j=p(j)$ for a given sample opacity $\chi=\kappa_0^{(L)}R$ via the mode resonance conditions (11). The function $\Delta S(p)$ entering Eq. (11) is the phase jump due to quasiparticle reflection at the boundary of the volume Ω_{Sh} [18]. Equation (11) establishes also a relationship $\chi(p,j)$ between MOT opacity χ and quasiparticle momentum p. In combining $\chi(p,j)$ with the explicit dependence $g(p)=\lambda^{-1}(p)$ of the trapping factor on p presented by Eq. (9), we obtain parametric form of g_j as a function of the opacity χ convenient for practical plotting (see Figs. 2 and 3). Note that the momentum enters all formulas as the dimensionless ratio $\chi_r=\kappa_0^{(L)}/p$, which may be considered as a reduced opacity. As is seen from Eq. (11), higher modes have smaller values of their individual opacity $\chi_r^{(j)}=\kappa_0^{(L)}/p_j$, so that $\chi_r^{(j)}\to 0$ with $j\to\infty$. For this reason the trapping factor g_j is a decreasing function on the mode index [Fig. 3(b)] and drops into unit value for $j=\infty$.

V. RESULTS AND DISCUSSION

The quantum number $j=0$ corresponds to the fundamental mode and the factor $g_0=\lambda_{p_0}^{-1}$ determines the delay in the radiative decay process due to RI at late times, when higher modes ($j>0$) have disappeared. Experimental values of g_0 have been evaluated from fluorescence decay curves (see, e.g., Fig. 1) according to the best fit procedure mentioned in Sec. II. So-determined g_0 factors obtained in Cs and Rb experiments under probe excitation at zero detuning ($\delta=0$) are plotted as a function of the MOT opacity χ in Fig. 3(a). Since the accuracy of the experimental evaluation of g_0 relies on the circumstance that only the fundamental mode $j=0$ survives for the data considered in the best fit, the behavior expected for the higher modes is worthy to be considered. Figure 3(b) shows the trapping factors for $j=0,1,2$ calculated according to our approach (based on the SCS model) as a function of the MOT opacity χ. Trapping factors for higher modes appear to be much smaller than for the fundamental mode in all the opacity ranges explored in our experiments. Furthermore, our analysis allows us to estimate the time of the decay process starting from which higher modes can be neglected as $\sim\tau_{ef}=g_0/\Gamma$ that roughly corresponds to the criterion applied in fitting experimental data (see Sec. II).

Superimposed to experimental data in Fig. 3(a) are the results of our calculations for g_0 (solid line, indicated as SCS in the legend). A rather good agreement is obtained in the whole opacity range explored. The same figure displays also calculations based on the model of Payne *et al.* [15] (dashed line) and results obtained assuming complete frequency redistribution with a Lorentz line profile (dotted line, denoted as CFR in the legend). For small opacities, SCS and CFR values of trapping factors are close to each other. For large opacities, the following asymptotical expressions are available with the above discussed GQT (Sec. IV) for spherical geometries:

$$g_0^{(SCS)}\simeq\frac{9}{8\pi^2}\chi^2,\quad g_0^{(Ch)}\simeq\frac{3}{\pi^2}\chi^2,\quad g_0^{(CFR)}\simeq\frac{\sqrt{\pi\chi}}{1.34}. \tag{12}$$

In other words, when increasing atom density, SCS behavior exhibits the χ^2 dependence typical for coherent radiation scattering (Ch) occurring under Milne's treatment of RI [1]. It is noteworthy that the coherent scattering is reproduced under MOT conditions by the results based on the model of Payne *et al.* [15]. On the other hand, calculations demonstrate a marked difference between SCS and Payne *et al.* results under the conditions of our experiments. They indicate as well that implementation of complete frequency redistribution leads to g_0 factors remarkably smaller than those measured in the MOTs.

Numerical description of the entire fluorescence time behavior needs special techniques for solving nonlinear radiation trapping problems [3]. Indeed, the intensity of the probe laser used in the experiment was large enough to provide partial saturation of the vapor and, thus, to decrease the effective absorption coefficient. The total flux J of fluorescence emerging from the MOT is directly connected with the total number of excited atoms $\bar{N}^*(t)=\int_{\Omega_{Sh}}d^3rn^*(r,t)$: $J=-d\bar{N}^*(t)/dt$. The following closed system of balance equations can be written to evaluate $\bar{N}^*(t)$:

$$\frac{d\bar{N}^*}{dt}=-\frac{\Gamma\bar{N}^*}{g_0(\chi(t))},\quad \frac{\chi(t)}{\chi}=\left[1-\frac{\bar{N}^*(t)}{\bar{N}_s^*}\right]\left[1-\frac{5}{9}\frac{\bar{N}^*(t)}{\bar{N}_s^*}\right]. \tag{13}$$

The set of not very restrictive assumptions leading to such a closed system of equations is discussed in detail in Ref. [3]. Briefly, it is required that (i) the whole MOT volume is crossed by the laser beam homogeneously, (ii) the probe laser detuning is zero, (iii) a two-level atom model is considered, (iv) collisional quenching and broadening are negligible, and (v) the probe laser pulse must be strong enough to cause appreciable saturation of the resonance transition, but, at the same time, its intensity has to be low enough that high-field effects (e.g., ac-Stark splitting) remain negligible.

The physical meaning of the system of Eq. (13) is as follows. The effective decay rate of excited atoms depends on the current MOT opacity $\chi(t)$, which, in turn, is determined by the current value of $\bar{N}^*$. If the initial saturation was complete, i.e., the excitation of the MOT vapor by the probe laser pulse got the maximum allowed value $\bar{N}_s^*$ ruled by the normal atoms concentration N and level degeneracies [3], the sample would become transparent, with $\chi(t=0)=0$. For low excitation power, $\bar{N}^*/(\bar{N}_s^*)\ll 1$ at a later stage of the decay process, the opacity $\chi(t)$ acquires its maximum value $\chi=\kappa_0^{(L)}R$. Results of our fluorescence signal evaluations based on solution of Eq. (13) are superimposed on experimental data in Fig. 1, which confirms the validity of our treatment in reconstructing the whole process dynamics.

Data discussed so far deal with a probe laser in resonance with the transition, i.e., with zero detuning. We stress that, by changing the probe laser detuning, initial (i.e., excitation) conditions are modified. However, as we will discuss in the following, manipulation of the initial conditions turns out to affect the whole RI process in our MOTs. Moreover, analysis of RI features as a function of the detuning provides us with essential insights into the basic mechanisms of radiative transfer in our experimental conditions.

Let us start by studying the frequency part of the spectral problem, i.e., let us consider calculations of the mode emission profiles $\varphi_p(\nu)$ determined by Eq. (9), presented in Fig. 4. The modes have individual values of the momentum p_j and, accordingly, of the reduced opacity $\chi_r^{(j)}$, which are found from resonance conditions, Eq. (11). As it was mentioned above (Sec. IV), higher modes acquire smaller opacities $\chi_r^{(j)}$ provided the sample optical thickness χ is fixed in the experiment. The modes, thus, possess different spectral emissivity that has to result in some relaxation processes occurring in the frequency space for optically dense MOTs. To justify the latter statement and, at the same time, to understand the trend of the curves depicted in Fig. 4, it is worthwhile to describe the limiting profile shapes $\varphi_p^{(sm)}(\nu)$

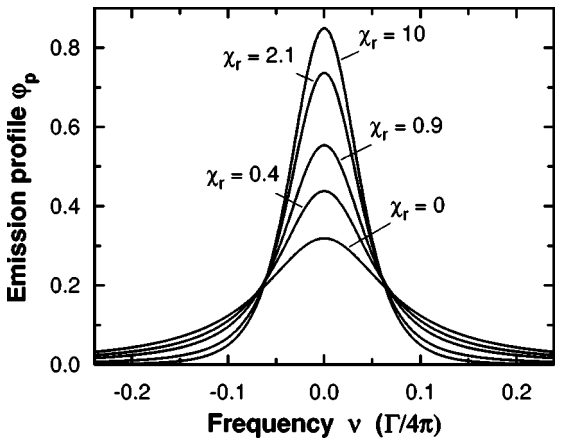

FIG. 4. Emission profiles $\varphi_p(\nu)$ of the modes calculated as a function of the frequency ν for different reduced opacities χ_r of the modes, as indicated in the plot. The frequency is measured from the line center ν_0 in units of the Lorentz width $\Gamma/4\pi$.

and $\varphi_p^{(lar)}(\nu)$, at small and large opacities ($\chi_r \ll 1$ and $\chi_r \gg 1$, respectively):

$$\varphi_p^{(sm)}(\nu) \simeq \frac{1}{\pi}\frac{1}{1+\nu^2}, \quad \varphi_p^{(lar)}(\nu) \simeq \frac{8}{3\pi}\frac{1}{(1+\nu^2)^3}. \quad (14)$$

For a low-opacity MOT, the emission profile has a Lorentz character, while in the other limit the profile is essentially narrower, as seen in Fig. 4, and acquires a new power dependence ($\propto \nu^{-6}$) in the wings. The fundamental mode ($j=0$) exhibits a larger value of the reduced opacity $\chi_r^{(j=0)}$ as compared with other modes ($j>0$). Thus, the initial frequency curve of the fluorescence signal tends to relax into the narrower profile $\varphi_{p=p_0}(\nu)$ at the later stage of the decay process when the fundamental mode survives. Nevertheless, the corresponding fluorescence broadening $\Delta\omega_{fl}$ (angular frequency units) remains always greater than zero; indeed it exceeds the full-width at half-maximum bandwidth ($\simeq 2 \times \Gamma/4$) of the $\varphi_p^{(lar)}(\nu)$ profile also at late times of the decay. This can be interpreted as some ''memory'' mechanism conserving (during the decay stage) the radiative broadening Γ' of the initially formed (during the excitation stage) fluorescence line at the approximate level of $\Gamma/2$. Importantly, existence of the residual bandwidth $\Delta\omega_{fl} \geqslant \Gamma/2$ turns out to be a feature inherent to the SCS model. Under the frame of Payne treatment (coherent scattering), the fundamental mode has the spectral emissivity in the form of $\delta(\nu - c/\lambda)$ with zero width.

Furthermore, we note that the spectral distribution $P_{ex}(\omega)$ of a weak radiation field formed in the MOT volume due to the fluorescence of decaying modes can be found from the convolution theorem [23] as well: $\varphi_p(\omega) = P_{ex}(\omega)(1 + 4\omega^2/\Gamma^2)^{-1}$. The bandwidth $\Delta\omega_{ex}$ of the radiation, thus, appears to exceed always the natural width Γ in SCS model. It can be seen also that the requirement ''the product of the bandwidth of the radiation and the time scale over which the intensity changes is much larger than unity'' (i.e., $\Delta\omega_{ex}\tau_{ef} \gg 1$) [24], formulated in Ref. [11] for the implementation of the SCS equation, is satisfied in the case of strong enough

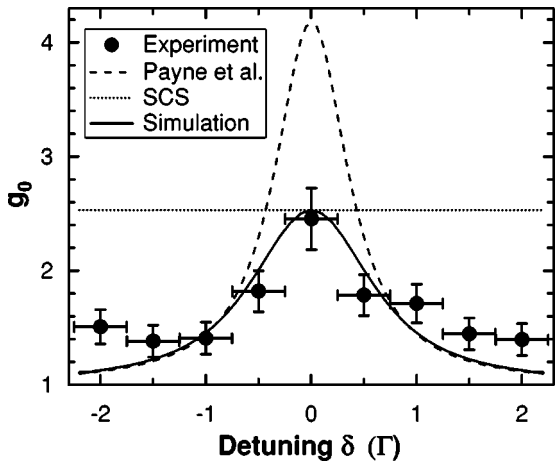

FIG. 5. Dependence of trapping factor g_0 of the fundamental mode on the probe laser frequency detuning δ (angular frequency units) in the Rb MOT with $\chi = 2.4$. The detuning is measured in units of Γ. Experimental data are reported as closed circles. The dashed line represents the g_0 factors according to the model of Payne *et al.* [15], the dotted straight line is the constant value provided by the SCS model in the conditions of the experiment. The solid line corresponds to our ''simulation'' obtained as discussed in the text.

imprisonment and detuning below $\Gamma/2$. In other words, Eq. (2) remains valid even in the decaying stage of our experiments, when no broadening is stimulated by external radiation sources. In this sense, as anticipated above, the initial conditions affect the whole RI process. The situation changes dramatically in the dispersive part of the line profile (probe laser detuning above $\Gamma/2$), where virtual processes play the main role and scattering events become strongly influenced by the field strength. The inequality $\tau_{ef} > \tau_{sc}$ is obviously not fulfilled here, and it is hard to expect adequacy of the SCS model to the experiment.

It is noteworthy that in the low opacity regime we need larger probe laser intensities ($s \sim 3$) to satisfy the inequality $\tau_{ef} > \tau_{sc}$. If we fix both opacity $\chi = 2.4$ and the saturation parameter $s = 3$ in the Rb experiment and then we start detuning the probe laser frequency, the above inequality breaks down approximately for $s(\delta) < 2.4$, i.e., at probe laser detuning $|\Delta| = |\delta|/\Gamma > 0.25$. Thus, by simply tuning the probe laser frequency we can have direct experimental access to a regime where the model based on SCS is expected to loose validity. Figure 5 displays the g_0 factor measured at different detuning values of the probe laser in the Rb MOT experiment. We recall that in the SCS model no strong dependence of initial conditions on the detuning is expected, due to the Markov-like (instantaneous) character of scattering processes [11]. Formally, it means a dominant excitation of the fundamental mode ($j=0$) occurs, regardless of the frequency of the probe laser. We have represented such a circumstance in the figure, where a straight dotted line (at the value calculated for the actual conditions of the experiment) shows the expected behavior of g_0 factor according to the SCS model. On the contrary, the approach by Payne *et al.* [15] implies independent decay of different frequencies in the fluorescence signal, thus predicting a dependence on the detuning.

This leads, in the conditions of our experiment, to the dashed line displayed in the figure.

It is well seen that both SCS and Payne *et al.* equations are unable to describe properly the experimental results outside the region of validity. Nevertheless, it is possible to achieve a satisfactory agreement with the experiment by combining the characteristic properties of both treatments in some kind of a ''mixed'' model; namely, Eq. (10) implies that evaluation of effective radiative constants λ_j can be reduced to the Holstein equation provided one has *a priori* information on the emission profile $\varphi(\nu)$ in the j mode. We simulated RI features as a function of the detuning having assumed that during the decay stage the excited atoms emission profile $\varphi(\nu)$ remained homogeneous in the MOT volume and preserved: (i) its initial radiative broadening Γ' (the main feature of SCS model); (ii) its initial carrier frequency (the main feature of Payne *et al.* model): $\varphi(\omega) \sim [\Gamma'^2 + 4(\omega - \omega_0 - \delta)^2]^{-1}$. The results of trapping factor calculations for the fundamental mode in a such ''simulation'' are displayed in Fig. 5 (solid line). Even if experimental data are affected by a relatively large uncertainty, ascribed to fluctuations in MOT and probe laser operation, they are relatively well recovered by the curve.

VI. CONCLUSIONS

We have derived explicit analytical results of RI in cold atom samples by modeling it as a Markov-like process using SCS equation and applying GQT for its solution. Our results, confirmed through comparison with experimental findings, shed light on nonstationary radiative transfer in cold atomic samples, and can be useful, for instance, in diagnosing the MOT average density. On the other hand, they demonstrate that special care must be devoted to define the operating regime, i.e., to identify correct theoretical assumptions for the specific conditions of the experiment. Indeed, we find that, in our experimental conditions, the SCS approach is no longer valid for probe excitation far from resonance. Our results as a function of the detuning suggest the occurrence of a transition regime where different processes that are nonlocal in time play a role in the radiative transfer.

Further work will be devoted to carry out experiments with larger probe laser intensity and sample opacity, which may lead to the observation of subnatural fluorescence decay [3] in cold atom systems. Furthermore, excitation with a tightly focused probe beam will be analyzed in order to stimulate competition processes in the dynamics of RI mechanisms, as predicted in Refs. [4,19]. Further theoretical work on the basis of Ref. [2] will also be undertaken that might lead to describe those experimental findings not interpreted in the present work.

ACKNOWLEDGMENTS

We thank Ennio Arimondo for illuminating discussions and a critical reading of the manuscript. We gratefully acknowledge support from the Italian Ministry of Foreign Affairs within the frame of Italo-Russian Agreement for Scientific and Technological Cooperation 2002-2004, Grant No. RB19, financial support from INTAS through Project No. 01-0155, and from NATO Science Program via Collaboration Linkage Grant No. PST.CLG.979120.

[1] A.F. Molisch and B.P. Oehry, *Radiation Trapping in Atomic Vapours* (Oxford University Press, Oxford, 1998).
[2] V. Makhrov, A.Yu. Sechin, and A.N. Starostin, Zh. Éksp. Teor. Fiz. **97**, 1114 (1990) [Sov. Phys. JETP **70**, 623 (1990)].
[3] N.N. Bezuglov, A.N. Klucharev, A.F. Molisch, M. Allegrini, F. Fuso, and T. Stacewicz, Phys. Rev. E **55**, 3333 (1997).
[4] A.K. Kazansky, N.N. Bezuglov, A.F. Molisch, F. Fuso, and M. Allegrini, Phys. Rev. A **64**, 022719 (2001).
[5] A.B. Matsko, I. Novikova, M.O. Scully, and G.R. Welch, Phys. Rev. Lett. **87**, 133601 (2001).
[6] T. Jonckheere, C.A. Müller, R. Kaiser, Ch. Miniatura, and D. Delande, Phys. Rev. Lett. **85**, 4269 (2000); C.A. Müller, T. Jonckheere, Ch. Miniatura, and D. Delande, Phys. Rev. A **64**, 033402 (2001).
[7] T. Walker, D. Sesko, and C. Wieman, Phys. Rev. Lett. **64**, 408 (1990); D.W. Sesko, T.G. Walker, and C.E. Wieman, J. Opt. Soc. Am. B **8**, 946 (1991).
[8] K. Ellinger and J. Cooper, Phys. Rev. A **55**, 4351 (1997).
[9] C. Cohen-Tannoudji, G. Grynberg, and J. Dupont-Roc, *Atom-Photon Interactions: Basic Processes and Applications* (Wiley, New York, 1998).
[10] H.J. Metcalf and P. van der Straten, *Laser Cooling and Trapping* (Springer-Verlag, New York, 1999).
[11] A. Streater, J. Cooper, and W. Sandle, J. Quant. Spectrosc. Radiat. Transf. **37**, 151 (1987).
[12] J. Cooper, R.J. Ballagh, K. Burnett, and D.G. Hummer, Astrophys. J. **260**, 299 (1982); J. Cooper and P. Zoller, *ibid.* **277**, 813 (1984).
[13] A. Fioretti, A.F. Molisch, J.H. Müller, P. Verkerk, and M. Allegrini, Opt. Commun. **149**, 415 (1998).
[14] C. Gabbanini, A. Fioretti, A. Lucchesini, S. Gozzini, and M. Mazzoni, Phys. Rev. Lett. **84**, 2814 (2000).
[15] M.G. Payne, J.E. Talmage, G.S. Hurst, and E.B. Wagner, Phys. Rev. A **9**, 1050 (1974).
[16] H.A. Post, Phys. Rev. A **33**, 2003 (1986).
[17] T. Holstein, Phys. Rev. **72**, 1212 (1947); **83**, 1159 (1951).
[18] N.N. Bezuglov, A.F. Molisch, A.N. Klucharev, F. Fuso, and M. Allegrini, Phys. Rev. A **57**, 2612 (1998).
[19] N.N. Bezuglov, A.K. Kazansky, F. Fuso, and M. Allegrini, Phys. Rev. A **63**, 042703 (2001).
[20] N.N. Bezuglov, A.K. Kazanskii, A.N. Klyacharev, K. Miculis, F. Fuso, and M. Allegrini, Opt. Spectrosk. **95**, 665 (2003) [Opt. Spectrosc. **95**, 631 (2003)].
[21] Hereafter the Planck constant is set equal to unity.
[22] Equation (10) is easily obtained after integration over the frequency ν of both sides in Eq. (6) with accounting for normalization identities, Eq. (3), and factorization property, Eq. (7).
[23] M.G. Raymer and J. Cooper, Phys. Rev. A **20**, 2338 (1979).
[24] This requirement coincides with our criterion $\tau_{ef} > \tau_{sc}$.